Article

Development of a Novel Sensitive and Fast Semi-Covalent Molecularly Imprinted Polymer-Based Magnetic Dispersive Solid-Phase Extraction Method (MIP-MDSPE) for Cholesterol Determination in Milk Samples

Luciane Effting, [a] *Alesandro Bail,* [b] *Mariana G. Segatelli* [a] *and César R. T. Tarley* [*,a,c]

aLaboratório de Desenvolvimento de Métodos Analíticos (LADEMA), Departamento de Química, Universidade Estadual de Londrina (UEL), 86057-970 Londrina-PR, Brazil

bGrupo de Química de Materiais e Tecnologias Sustentáveis (GQMATS), Universidade Tecnológica Federal do Paraná (UTFPR), 86036-370 Londrina-PR, Brazil

cInstituto Nacional de Ciência e Tecnologia de Bioanalítica (INCTBio), Universidade Estadual de Campinas (UNICAMP), 13083-970 Campinas-SP, Brazil

In the present study, a novel magnetic dispersive solid-phase extraction method using molecularly imprinted polymer synthesized through semi-covalent imprinting approach was developed for cholesterol (CHO) determination in milk samples by high-performance liquid chromatography with diode array detector (HPLC-DAD). The adsorbent named $Fe_3O_4/SiO_2/MIP$ (MIP: molecularly imprinted polymers) was prepared through sol-gel polymerization of 3-(triethoxysilyl)propyl isocyanate (ICPTES) covalently bonded to CHO with tetraethoxysilane (TEOS), in the presence of Fe_3O_4/SiO_2 particles. The adsorbent was characterized by attenuated total reflection Fourier transform infrared (ATR-FTIR), X-ray diffraction (XRD), dynamic light scattering (DLS) and scanning electron microscopy (SEM). The proposed molecularly imprinted polymer-based magnetic dispersive solid-phase extraction method (MIP-MDSPE) was based on vortex-assisted preconcentration of 10.0 mL of CHO solution in chloroform as donor phase using 10.0 mg of $Fe_3O_4/SiO_2/MIP$ during 60 s. After this step, the magnetic particles were collected using a permanent magnet and the vortex-assisted elution was carried with 500 μL of ethanol during 180 s. A wide analytical curve ranging from 38.5 to 25000 μg L^{-1} (determination coefficient (R^2) = 0.998) and low limits of detection (LOD) and quantification (LOQ) 11.5 and 38.5 μg L^{-1}, respectively, were obtained. Milk samples (whole and reduced-fat milk) were subjected to MIP-MDSPE method after saponification reaction followed by CHO extraction with chloroform. Using external calibration, the CHO concentration ranged from 99.2 (reduced-fat milk) to 397.6 mg kg^{-1} (whole milk) and the accuracy was attested by addition and recovery tests (92 to 97%).

Keywords: milk samples, magnetic separation, polymer magnetic, liquid chromatographic, saponification

Introduction

Cholesterol (CHO) has a fundamental function in the human body, being a precursor in the synthesis of other essential compounds to human health and with activity in the interior of cell membranes.[1] Some studies have reported that high serum CHO might be a predictor for cardiovascular events in young adults, although there is no strong evidence to support the association of dietary cholesterol with cardiovascular diseases.[2] In addition, epidemiological data and clinical studies indicate that there is not a direct correlation between CHO intake and serum CHO.[3,4] From these studies, it is clearly demonstrated that more in-depth research on the dietary CHO needs to be done. Anyway, it is very well known that diet plays an important role in overall health and heart health. Until 2010, the Dietary Guidelines for Americans Trusted Source[5] limited the maximum level of CHO intake to no more than 300 mg *per* day. However, nowadays the same guideline does not establish a specific limit but recommends the intake of food with low CHO content.[5]

Considering that major intake sources of CHO are milk, meat, eggs, and their derivatives, and the high consumption

of these foods among the overall population, it is crucial the quantification of CHO for assessing the nutritional quality. In addition, due to complexity of food matrices,[6-9] the development of novel fast, selective, and sensitive analytical methods is of paramount importance.

The developed method by Al-Hasani *et al.*[10] has still been widely used for determining CHO in foods, which involves alcoholic KOH saponification under reflux (1 h) of the sample following the liquid-liquid extraction of CHO with large amounts of hexane, with posterior determination by gas chromatography using 5-α-cholestane as internal standard. This method is time-consuming and makes use of large amounts of toxic solvent.

Currently, more environmentally friendly methods based on dispersive liquid-liquid microextraction (DLLME),[11] magnetic dispersive micro solid-phase extraction combined with supramolecular solvent-based microextraction (Mdμ-SPE-SSME)[12] and molecularly imprinted solid-phase extraction (MISPE)[13-15] have been developed for food sample clean-up and/or CHO preconcentration. Undoubtedly, molecularly imprinted polymers (MIP) as selective extractor adsorbents have been increasingly used in the field of separation science, due to their intrinsic selectivity toward the target analyte used in the synthesis as template molecule.[16,17]

As well known, the selective and adsorptive performance of MIPs depends upon the synthesis approach, morphology of adsorbent as well as the modality of preconcentration method. In this sense, in the semi-covalent imprinting approach, the template is covalently bound to the functional monomer during polymerization process followed by the removal of the template. In the rebinding process, only non-covalent interactions are exploited. This synthesis method is particularly useful for relatively large template molecules, such as CHO, which contains only one binding site, and can provide more selective sites with high binding capacity due to better integrity of binding sites obtained in the polymerization compared with non-covalent imprinting approach.[18,19]

The use of MIPs in the development of preconcentration methods exploiting magnetic dispersive solid-phase extraction (MDSPE) is another successful strategy for improving the performance of MIPs. In this technique, the contact area between adsorbents and analytes is large since the adsorbent can be uniformly dispersed into the sample solution, allowing a quick mass transfer and a shorter extraction time. In 1998, Ansell and Mosbach[20] reported the first use of a magnetic MIPs, in which a MIP for (*S*)-propranolol was polymerized on the surface of the magnetic iron oxide and since then, this material has been applied to environmental,[21-23] food,[24-26] and biological samples.[27-29] Magnetic MIPs are basically synthesized with

core-shell structure, where the core is the magnetic particle, usually Fe_3O_4, the shell is the thin polymeric layer of MIP supported on the surface of core. Such adsorbent provides a quick adsorption process once the imprinted cavities are accessible on the thin polymeric layer,[30] but the number of selective imprinting binding sites is relatively low. For this reason, magnetic MIPs can also be prepared by the formation of interpenetrating magnetic particles in a large polymeric network, giving rise, in principle, to adsorbents with higher adsorption capacity as result of greater amount of selective binding sites.

According to aforementioned, this study deals with the first time the practical feasibility of magnetic MIP synthesized through semi-covalent synthesis and sol-gel process in the development of a MDSPE method for cholesterol determination in milk samples by high-performance liquid chromatography with diode array detector (HPLC-DAD).

Experimental

Reagents and solutions

All reagents used in the synthesis of materials were of analytical grade and purchased from Sigma-Aldrich (St. Louis, MO, USA): cholesterol (CHO), iron(III) chloride hexahydrate ($FeCl_3.6H_2O$) and iron(II) chloride tetrahydrate ($FeCl_2.4H_2O$), sodium metasilicate pentahydrate ($Na_2SiO_3.5H_2O$), tetraethoxysilane (TEOS), 3-(triethoxysilyl)propyl isocyanate (ICPTES), dimethylsulfoxide (DMSO), tetrahydrofuran (THF), ethanol (EtOH), hydrochloric acid (HCl), sodium hydroxide (NaOH). Reagents used in the experiments were of analytical grade: chloroform ($CHCl_3$), methanol (MeOH), ethanol (EtOH), acetonitrile (ACN) were purchased from Sigma-Aldrich. For the mobile phase in chromatographic determination, acetonitrile (ACN) was purchased from Sigma-Aldrich (St. Louis, MO, USA) and ultrapure water was obtained from an ELGA PURELAB system (High Wycombe, Bucks, UK).

Instruments

Cholesterol was determined using a liquid chromatograph model LC-20AT, Shimadzu Prominence, Tokyo, Japan. A CLC-ODS column (250 mm × 4.6 mm i.d. (internal diameter), 5 μm in particle size) and a guard column Phenomemex (4.0 mm × 3.0 mm i.d., 5 μm in particle size) were used. The peak purity was determined on a diode array detector (DAD) and monitored at $\lambda_{max} = 210$ nm. The flow rate of the mobile phase consisting of acetonitrile (ACN) and

water (9:1, v/v) was 1.0 mL min^{-1}, operating isocratically and the injection volume was 20.0 µL. The temperature of the chromatographic separation (30 °C) was controlled by using a column oven. Attenuated total reflection Fourier transform infrared (ATR-FTIR) analysis was carried out on a Bruker Vertex 70 (Bruker Optics, Rheinstetten, Germany), with platinum ATR reflectance accessory in the range 400-4000 cm^{-1}. Spectra were collected with a resolution of 4 cm^{-1} and an accumulation of 16 scans. X-ray diffraction measurements were carried out through self-oriented films placed on glass sample holders. The measurements were performed in a Shimadzu XRD-7000 (Hertogenbosch, Netherlands) diffractometer operating at a voltage of 30 kV and a current of 40 mA (Cu Kα radiation λ = 0.15418 nm). The average particle size analysis was performed by the dynamic light scattering (DLS) technique using a Microtrac MRB's NANOTRAC Wave II (Microtrac Retsch GmbH, Haan/Duesseldorf, Germany) instrument, equipped with a 780 nm and 3 mW laser source. For this task, the samples of Fe_3O_4, Fe_3O_4/SiO_2 and $Fe_3O_4/SiO_2/MIP$ were suspended in ethanol (1 mg mL^{-1}). All measurements were taken at a detection angle of 180º and the reported sizes are all averages from 3 sequential runs of 30 s each. The instrument was previously calibrated with a Microtrac 100 nm Polysphere Reference Kit. Scanning electron microscopy (SEM) was recorded in an FE-SEM (TESCAN) model MIRA 3 LMU (Brno, Kohoutovice, Czech Republic). Before the analysis, the samples were placed in an aluminum sample port fixed with carbon tape and metalized with gold. Optical microscope images were recorded in an Hund Wetzlar model V300 (Helmut Hund GmbH, Wetzlar, Germany). Magnifications were obtained with an ocular lens (10×) and objective lens (40 and 100×). The final magnifications were 400 and 1000×.

Preparation of Fe_3O_4/SiO_2

The synthesis and modification of magnetite nanoparticles (Fe_3O_4) were performed by the co-precipitation method.[19] In a three-neck round-bottom flask, 10.8 g of $FeCl_3.6H_2O$ was mixed with 25.0 mL of 1.0 mol L^{-1} HCl and 25.0 mL of degassed distilled water. The mixture was kept in a silicon bath at 60 ºC under an N_2 atmosphere. In another flask, 25.0 mL of degassed distilled water was mixed with 3.97 g of $FeCl_2.4H_2O$ and kept under an N_2 atmosphere. Afterward, the $FeCl_2.4H_2O$ solution was slowly added to the $FeCl_3.6H_2O$ one under magnetic stirring and under N_2 flow. Next, 250.0 mL of 1.5 mol L^{-1} NaOH was slowly added to the mixture and kept under magnetic stirring for 40 min at 60 ºC. Upon synthesis, a neodymium magnet was used to separate the magnetic particles, which were further exhaustively washed with

deionized water until a pH 7.0. The obtained particles (2.0 g) were dispersed in 200.0 mL of deionized water, followed by the addition of 0.04 mol of $Na_2SiO_3.5H_2O$, 1.0 mol L^{-1} HCl to adjust the pH to 7.0, and left to completely react for 3 h at 60 °C under N_2 atmosphere and magnetic stirring. Finally, the material was washed with deionized water and dried at 60 °C overnight. The solid was labeled Fe_3O_4/SiO_2.

Preparation of the template-monomer covalently bonded (CHO-IPTES)

The covalent bond of CHO with ICPTES (CHO-ICPTES) was carried using 3.0 g of template CHO (cholesterol, 7.75 mmol) and functional monomer 5.44 mL of ICPTES (3-(triethoxysilyl)propyl isocyanate, 27.0 mmol) dissolved in 30.0 mL of anhydrous tetrahydrofuran (THF).[19] The reaction mixture was magnetically stirred at 60 °C for 24 h under a nitrogen atmosphere. After the reaction, the solvent was evaporated under vacuum and the CHO-ICPTES product was obtained.

Preparation of $Fe_3O_4/SiO_2/MIP$

In a flat-bottom flask, 1.5 g of Fe_3O_4/SiO_2 nanoparticles were ultrasonic-assisted dispersed in 30.0 mL of MeOH. Under stirring, 1.0 g of CHO-IPTES, 6.0 g of TEOS (28.0 mmol), and 1.5 mL of HCl (1.0 mol L^{-1}) were added to mixture and kept under stirring for 12 h at room temperature. The product, named $Fe_3O_4/SiO_2/MIP$-CHO was separated by an external magnetic field, washed with ethanol, and deionized water, and then dried at 60 °C. In order to remove the template molecule, $Fe_3O_4/SiO_2/MIP$-CHO was added to a solution containing dimethylsulfoxide (DMSO) and deionized water (5:1, v/v, respectively) and the mixture was refluxed at 160 ºC for 8 h. Then, the product, named $Fe_3O_4/SiO_2/MIP$, was isolated by an external magnetic field and washed alternately with ethanol and deionized water three times each. Finally, the magnetic material was dried in an oven at 60 ºC overnight.

Molecularly imprinted polymer-based magnetic dispersive solid-phase extraction (MIP-MDSPE) procedure

The MIP-MDSPE procedure was based on vortex-assisted preconcentration during 60 s of 10.0 mL of standard CHO solution in chloroform medium in the presence of 10 mg of $Fe_3O_4/SiO_2/MIP$. It is important to point out that chloroform, hexane, H_2O/methanol, methanol, ethanol, and acetonitrile were previously evaluated as medium for CHO adsorption on the $Fe_3O_4/SiO_2/MIP$,[19] being the chloroform the best solvent. For more details regarding this study and

selectivity performance of adsorbent can be found in the literature.[19] Additionally, as chloroform was chosen as the best solvent because it was used for extraction of CHO from unsaponified sample. After extraction, the magnetic nanoparticles containing CHO adsorbed were collected with a neodymium magnet and the elution was carried out with 500 μL of ethanol during 180 s vortex-assisted. The eluent was evaporated to dryness dissolved in the mobile phase and analyzed by HPLC-DAD. The scheme of MIP-MDSPE procedure is depicted in Figure 1.

Analytical parameters of MIP-MDSPE procedure

Analytical parameters including analytical curve, intra-day and inter-day precision, limit of detection (LOD), limit of quantification (LOQ)[31] and preconcentration factor (PF) were determined under the optimized conditions. The analytical curve was ranged from 50.0 to 25000 μg L^{-1} and the LOD and LOQ were determined as 3std/m and 10std/m, respectively, where std is the standard deviation from 10 measurements of blank and m is the slope of analytical curve. The analytical curve obtained without preconcentration step was range from 2000 to 300.000 μg L^{-1} and the PF was determined calculated as the ratio between the slopes of analytical curves obtained with and without the preconcentration step.[32] The intra-day and inter-day precision (two consecutive working days) was assessed in terms of repeatability by analyzing (n = 10) cholesterol concentrations of 5000 and 10000 μg L^{-1} and the relative standard deviations (RSD) were determined.

Preconcentration and clean-up of total cholesterol from the cow milk

Whole and reduced-fat UHT (ultra-high temperature) cow milk samples were acquired from a local supermarket in Londrina (Brazil). 10.0 g of the milk was accurately weighed and placed in a 50.0 mL flask. Then, 8.0 mL of 50% KOH solution and 12.0 mL of ethanol were added to the sample and thoroughly mixed.[10] Subsequently, the flask was placed in a water bath under stirring until complete solubilization of the sample for 10 min at 40 °C. In the next step, 10.0 mL of water and 3 × 10.0 mL of chloroform were added to the unsaponified supernatant.[33] The mixture was separated in a separatory funnel, and the chloroform extract was submitted to the procedure of MIP-MDSPE procedure. The extractions were performed in triplicate.

Results and Discussion

Characterization of adsorbent materials

ATR-FTIR

Initially, ATR-FTIR was used for confirming the formation of CHO-ICPTES. Figures 2a, 2b and 2c show, respectively, the spectra of CHO, ICPTES and CHO-ICPTES. The bands attributed to the hydroxyl group (–OH) in cholesterol at 3400 cm^{-1} and isocyanate group (–N=C=O) of ICPTES at 2263 cm^{-1} showed an intensity decrease, and the band belonging to the carbonyl group (1729 cm^{-1}) of CHO-ICPTES appeared in the spectrum (Figure 2c). This finding confirms the formation of CHO-ICPTES. The band at 1081 cm^{-1} is attributed to the siloxane group (Si–O), present in ICPTES in the CHO-ICPTES spectrum, indicating that ethoxy groups of the ICPTES remained unhydrolyzed after the reaction.[34]

ATR-FTIR spectra of Fe$_3$O$_4$ and Fe$_3$O$_4$/SiO$_2$ are shown in Figures 2d and 2e, respectively. A characteristic band can be identified in 3558 cm^{-1} related to O–H stretching due to the residual water molecules. For Fe$_3$O$_4$, it was possible to verify characteristic bands at 570 cm^{-1}, attributed to Fe–O stretching vibration, which indicated that Fe$_3$O$_4$ magnetic nanoparticles had been successfully synthesized.[35] For Fe$_3$O$_4$/SiO$_2$, beyond characteristic Fe$_3$O$_4$ bands, Si–O–Fe bands were also confirmed by the vibration at 448 cm^{-1}, the strong band at 1064 cm^{-1} and band at 794 cm^{-1} attributed to Si–O–Si asymmetric and symmetric stretching vibrations, respectively, and at 974 cm^{-1} a small shoulder is observed, attributed to the symmetrical stretching of silanol group (Si–OH), which indicated that the silicon layer was successfully formed on the surface of Fe$_3$O$_4$ magnetic nanoparticles.[35,36]
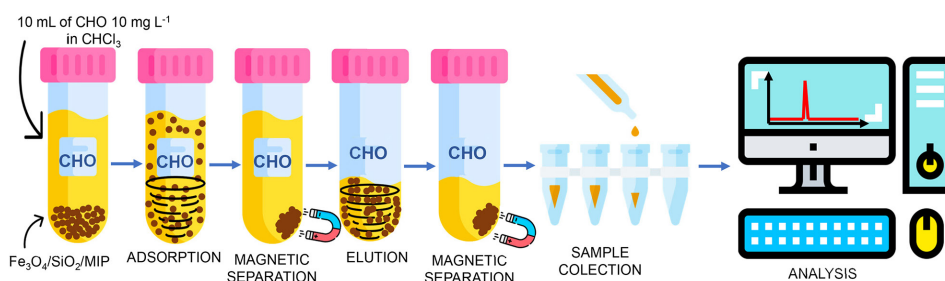
Figure 1. Scheme of MIP-MDSPE procedure using Fe$_3$O$_4$/SiO$_2$/MIP.

For the ATR-FTIR spectrum obtained for the adsorbent material, $Fe_3O_4/SiO_2/MIP$ shown in Figure 2f, in addition to the bands of Fe_3O_4 and Fe_3O_4/SiO_2, other characteristic bands of the functional groups expected to these materials were observed. The band at 3380 cm^{-1} corresponds to NH_2 and at 1640 cm^{-1} bending vibrations of N–H, indicating the formation of amino groups anchored at the surface of imprinted cavities after the chemical cleavage of urethane bonds between hydroxyl group of cholesterol and isocyanate group of ICPTES indicating the successful introduction of the functional groups in the imprinted cavities.[34,37,38]

X-ray diffraction (XRD)

The structural properties of synthesized materials were characterized by XRD. The XRD patterns of Fe_3O_4, Fe_3O_4/SiO_2 and $Fe_3O_4/SiO_2/MIP$ are displayed in Figure 3. In the 2θ range of 5-80°, six characteristic peaks for magnetite were observed for the three samples ($2\theta = 30.42$, 35.52, 43.53, 53.43, 57.46, and 62.80°). According to the JCPDS-International Center for Diffraction Data (JCPDS card: 19-629), the peak positions at the corresponding 2θ values were indexed as (220), (311), (400), (422), (511), and (440) diffraction planes of Fe_3O_4 suggesting the presence of magnetic phase in the composites.[39]

Fe_3O_4/SiO_2 and $Fe_3O_4/SiO_2/MIP$ exhibited an XRD pattern similar to uncoated Fe_3O_4. $Fe_3O_4/SiO_2/MIP$ presented a more evident halo-amorphous at 2θ range of 20-30° due to the higher amount of disordered silica on the surface of magnetite nanoparticles. Moreover, minor differences in peak width for the synthesized samples are observed, reflecting differences in particle size. The peak positions of samples remained unchanged, indicating that a step-by-step coating procedure did not cause any change in the crystalline structure of the magnetite, allowing strong ferrimagnetism, which was responsible for an easy separation from the reaction medium using an external magnetic field by a few seconds.

DLS analysis

Particle size measurements were performed by DLS analysis and shown in Table 1. The particle size value for Fe_3O_4 was similar to that reported in the literature.[40,41] After the silica coating, a decrease in particle size was observed, indicating that the silica coating on the magnetic nanoparticles protects the magnetic core, decreasing the aggregation and the interaction of the magnetic dipole of the particles. $Fe_3O_4/SiO_2/MIP$ showed a new particle size increase, indicative of adding layer and polymerization on the silica surface observed in SEM images.
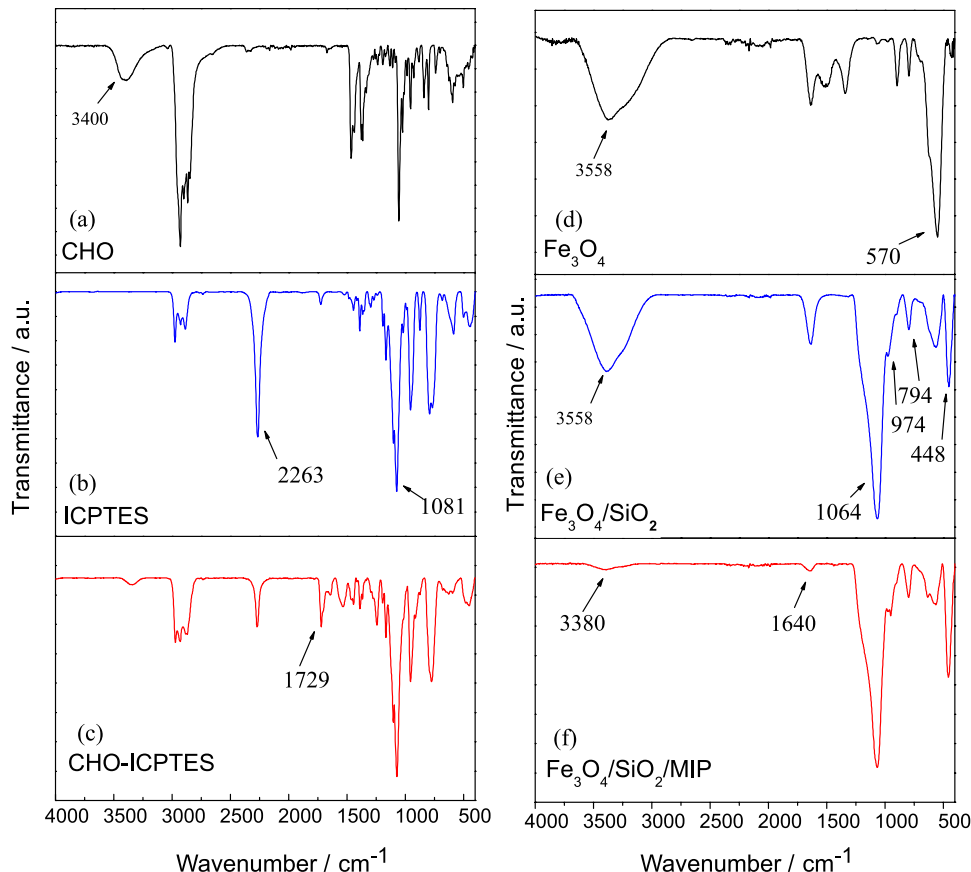
Figure 2. ATR-FTIR spectra of cholesterol (a), ICPTES (b), CHO-ICPTES (c), Fe_3O_4 (d), Fe_3O_4/SiO_2 (e) and $Fe_3O_4/SiO_2/MIP$ (f).
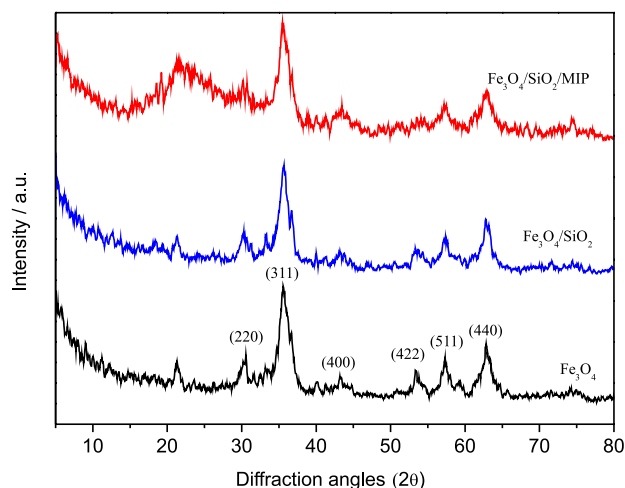
Figure 3. X-ray diffraction patterns of Fe_3O_4, Fe_3O_4/SiO_2, and $Fe_3O_4/SiO_2/MIP$.

The polydispersity (PdI) of the materials was higher as the number of coating layers increased. It is known that materials with a PdI below 0.5 suggest a monodisperse system, which was observed for Fe_3O_4 and Fe_3O_4/SiO_2. Thus, $Fe_3O_4/SiO_2/MIP$ was classified as a non-monodisperse system, showing PdI above 0.7. These results indicated that although coated materials have presented a lower level of aggregation, as their particle size suggests, the synthetic route for their coating caused the formation of covering layers of different thicknesses and, consequently, particles of distinct sizes. In addition, intermediate values ranging from 0.5 to 0.7 represent an approximate monodisperse system.[42]

Table 1. Size of the materials and polydispersity index measured by DLS technique

Material	Particle size / nm	Polydispersity index (PdI)
Fe_3O_4	579.0	0.0775
Fe_3O_4/SiO_2	242.6	0.441
$Fe_3O_4/SiO_2/MIP$	339.0	0.911

Scanning electron microscopy (SEM) and optical microscopy

SEM images show particle sizes with irregular shape, forming heterogeneous clusters and a rough surface (Figure 4). The aggregation of magnetic nanoparticles is due to the common magnetic dipole interactions for this type of material. It may lead to the formation of large aggregates that can exceed a few micrometers. Additionally, SEM images of $Fe_3O_4/SiO_2/MIP$ (Figure 4c) are a little different from those obtained for Fe_3O_4 and Fe_3O_4/SiO_2, visualizing the irregular shape of the Fe_3O_4 particles in the material is no longer possible, but larger

particles, irregular in size and shape and more cohesive, characteristic of the silica network formed via the sol-gel process.[39] This finding shows that a core-shell structure was not formed, instead occurred, as expected by synthesis approach, the formation of interpenetrating magnetic particles in a large polymeric network. The images from optical microscopy are shown in Supplementary Information (SI) section (Figures S1, S2 and S3). As observed, the particles present different sizes, which is in accordance with synthesis approach.

Optimization of MIP-MDSPE procedure

Different amounts of $Fe_3O_4/SiO_2/MIP$ were investigated (5.0, 10.0, 15.0, and 20.0 mg) for the CHO adsorption from 10 mL of 10 mg L^{-1} cholesterol solution in chloroform. As shown in Figure 5, 10.0 mg of $Fe_3O_4/SiO_2/MIP$ was enough for quantitative adsorption CHO, thus being chosen for posterior experiments.

The influence of solvent type, volume as well as the elution time vortex-assisted on the MDSPE has a vital role for avoiding memory effect during preconcentration and elution steps. This study was performed with polar and protic solvents (MeOH and EtOH), which weaken hydrogen interactions among the hydroxyl group of cholesterol and the NH_2 group created upon the chemical cleavage of CHO-ICPTES in the $Fe_3O_4/SiO_2/MIP$, thereby reducing affinity and facilitating the elution process. In addition, ACN was also evaluated, and elution time was ranged from 60 to 180 s.

The results shown in Figure 6a indicate that MeOH and EtOH provided highest elution percentage using 180 s. This result suggests that the interaction involving cholesterol and binding sites of $Fe_3O_4/SiO_2/MIP$ occurs by means of formation of hydrogen bond between the amino groups of the functional monomer and the hydroxyl group of the cholesterol molecule. As results of MeOH and EtOH were very similar to each other, EtOH was chosen as the best elution solvent as a compromise with Green Chemistry concept.

The elution solvent volume was evaluated in the range 200-2000 μL, as shown in Figure 6b. According to the results, the quantitative CHO elution occurred by using at least 500 μL of EtOH. Thus, this condition was selected as the eluent volume for further experiments.

Analytical parameters of MIP-MDSPE procedure

Under the optimized MIP-MDSPE procedure, the regression equation obtained was found to be (PA, peak area) = 9066.95[CHO] – 2408.31 with determination
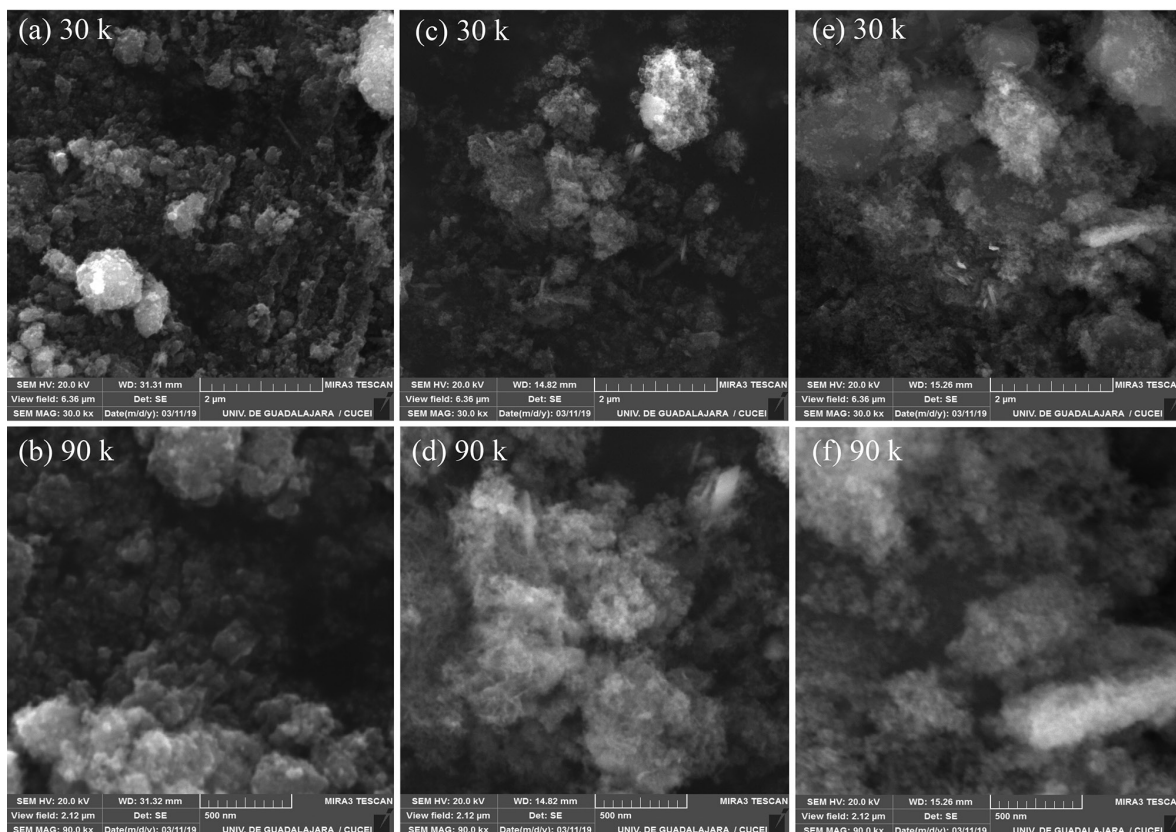
Figure 4. SEM images for the Fe_3O_4: (a) 30 and (b) 90 k, Fe_3O_4/SiO_2: (c) 30 and (d) 90 k, and $Fe_3O_4/SiO_2/MIP$: (e) 30 and (f) 90 k.
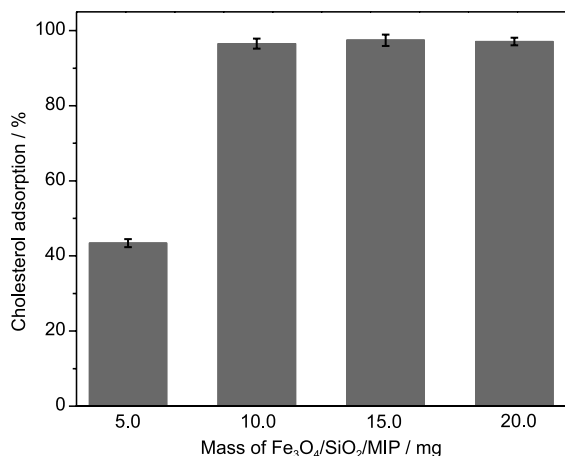
Figure 5. Influence of $Fe_3O_4/SiO_2/MIP$ mass on the cholesterol adsorption (%). Assays were carried out in triplicate.

coefficient (R^2) value of 0.998 in the range concentrations from 38.5.0 to 25000 µg L^{-1}. The regression equation obtained for the analytical curve without preconcentration step was found to be (PA, peak area) = 1149.14[CHO] − 7168.30 (R^2 = 0.997), giving rise to a PF of 7.8-fold. The LOD and LOQ were found to be 11.5 and 38.5 µg L^{-1}, respectively. The RSD values of intra-day precisions ranged from 1.60% (5000 µg L^{-1}, n = 10) to 1.52% (10000 µg L^{-1}, n = 10), which were indicative of high repeatability,

and the RSD values of inter-day precisions over two consecutive working days were lower than 2.50% for both concentrations.

Preconcentration and clean-up of total cholesterol from the cow milk

Three different milk brands were subjected to the MIP-MDSPE procedure after the saponification process.

The accuracy of proposed method was attested from addition and recovery tests ranging from 92 to 97%, using external calibration, which clearly indicates the absence of matrix effect and feasibility to determine cholesterol in cow milk (Table 2).

The determined values of CHO in this study are in agreement with literature data. However, it is important to point out that the cholesterol concentration in cow milk may be affected by species, breed, season, stage of lactation, and diet.[43] Gorban and Izzeldin[44] determined 256.0 mg kg^{-1} of CHO in cow milk, Bauer *et al.*[9] the range 42.8 to 88.7 mg kg^{-1} and Pietrzak-Fiecko and Kamelska-Sadowska[45] 205.8 mg kg^{-1}.

Figure 7 shows the chromatograms obtained with the direct injection of chloroform extract not purified by MIP-MDSPE and that was subjected to MIP-MDSPE.
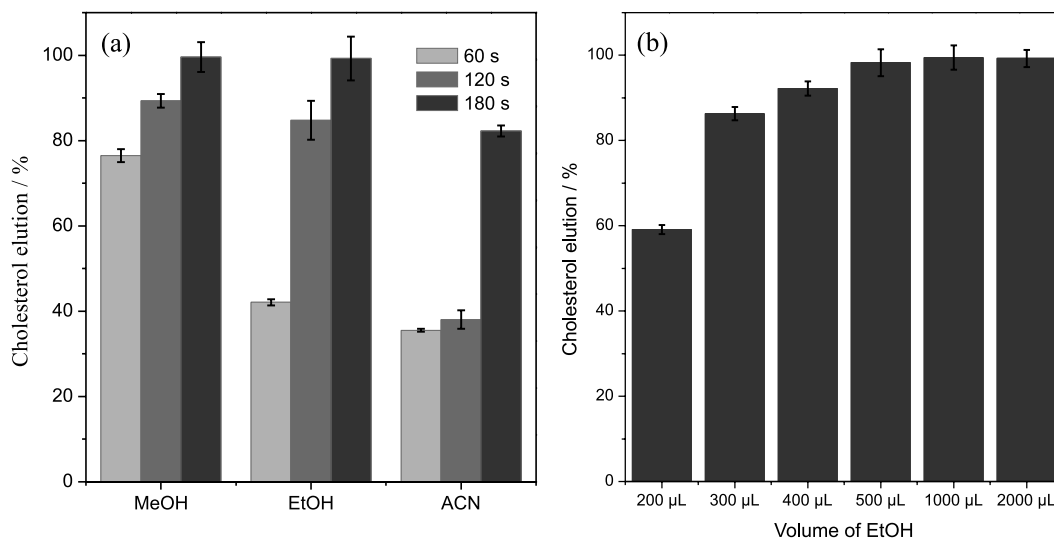
Figure 6. (a) Cholesterol elution (%) using 500 μL of MeOH, EtOH and ACN. (b) Cholesterol elution (%) with 200-2000 μL of EtOH. Conditions: 10 mL of 10 mg L^{-1} cholesterol solution in chloroform, mass of Fe$_3$O$_4$/SiO$_2$/MIP (10 mg). Assays were carried out in triplicate.

Table 2. CHO concentration determined in three different brands of UHT cow milk (n = 3) using MIP-MDSPE method

Milk	Added CHO / (mg kg^{-1})	Determined CHO^a / (mg kg^{-1})	Recovery / %
A (whole milk)	–	390.1 ± 0.1	–
B (whole milk)	–	397.6 ± 0.8	–
	30.0	426.7 ± 1.2	97
C (reduced-fat milk)	–	99.2 ± 0.1	–
	30.0	127.7 ± 1.1	95
	60.0	153.9 ± 1.0	92
	106.0	200.2 ± 1.3	95

^{a}The results are presented as mean ± standard deviation (n = 3).
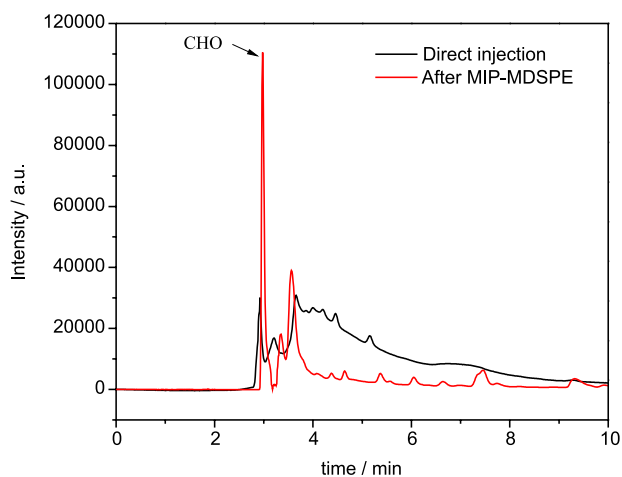
Figure 7. Chromatograms of the saponified extract injected directly and after the MIP-MDSPE.

As one can see, the intensity of CHO chromatographic peak for direct injection was lower when compared to the MIP-MDSPE. Moreover, using direct injection several

concomitants were observed in the chromatographic profile hindering the resolution of CHO peak. Therefore, the results clearly indicate the great importance of MIP-MDSPE proposed method for sample clean-up and improving the detectability of CHO in milk samples.

The proposed method was compared with other molecularly imprinted polymer solid-phase extraction-based methods previously published for the CHO determination in cow milk combined with HPLC-DAD and gas chromatography-flame ionization detector (GC-FID) (Table 3). As observed, the LOD (11.5 μg L^{-1}), the required time (240 s) for preconcentration and the mass of adsorbent were much lower than those already reported.

Conclusions

The Fe$_3$O$_4$/SiO$_2$/MIP was successfully synthesized and applied as a sorbent material in MIP-MDSPE to determine cholesterol in cow milk samples. The semi-covalent synthesis method was explored, employing a combination of a thermally reversible bond between template cholesterol and functional monomer ICPTES, which proved a simple procedure to create well-defined imprinted sites and achieve rapid target molecule interaction. The characterization techniques allowed the identification of functional groups created in the materials during the synthesis process. For Fe$_3$O$_4$/SiO$_2$/MIP, ATR-FTIR analysis confirmed the presence of amino groups which were created in the cleavage of the bond of cholesterol and ICPTES and are responsible for binding the cholesterol. The peaks referents of magnetite are predominated in XRD analysis for all synthesized materials, and images of SEM revealed an irregular morphology aspect. DLS analysis proved

Table 3. Comparison of LOD, sample volume and cholesterol determined in cow milk by HPLC-DAD and GC-FID

Sample	Extraction method	Clean-up/ preconcentration step	time required	Technique	LOD / (μg L^{-1})	Sample mass / g	Cholesterol removal from milk	Cholesterol range found / (mg kg^{-1})	Reference
Whole milk	MISPE	200 mg of MIP (molecularly imprinted poly(methacrylic acid)/silica hybrid)		HPLC-DAD	1210.0	10	30 mL of hexane	133.95-137.20	14
Whole milk	MISPE	350 mg of MIP PGMAT/PHEMA	2 h of adsorption and 2 h of elution	HPLC-DAD	59.0	0.8	8 mL chloroform: methanol 2:1 (v/v)	123.0	46
Whole milk	MISPE	100 mg of MIP (molecularly imprinted poly(methacrylic acid))	–	GC-FID	ca. 1000	10	25 mL of hexane	–	47
Whole and reduced-fat milk	MIP-MDSPE	10 mg of Fe$_3$O$_4$/SiO$_2$/ MIP	240 s	HPLC-DAD	11.5	10	30 mL of chloroform	390.07-397.61	this work

LOD: limit of detection; MISPE: molecularly imprinted solid-phase extraction; HPLC-DAD: high-performance liquid chromatography with diode array detector; PGMAT/PHEMA: poly(hydroxyethyl methacrylate) (PHEMA)-based cryogel with embedded cholesterol-imprinted poly(glycidyl methacrylate-*N*-methacryloyl-(L)-tyrosine methylester) (PGMAT); GC-FID: gas chromatography-flame ionization detector; MIP: molecularly imprinted polymers; MDSPE: magnetic dispersive solid-phase extraction.

an increase in particle size with the MIP layer. The MIP-MDSPE developed method proved to be efficient and fast for the quantification of CHO in milk samples, with satisfactory precision and accuracy attested from addition and recovery tests using external calibration.

Acknowledgments

References

1. Wadhera, R. K.; Steen, D. L.; Khan, I.; Giugliano, R. P.; Foody, J. M.; *J. Clin. Lipidol.* **2016**, *10*, 472. [Crossref]

2. Jeong, S.-M.; Choi, S.; Kim, K.; Kin, S. M.; Lee, G.; Park, S. Y.; Kim, Y.-Y.; Son, J. S.; Yun, J.-M.; Park, S. M.; *J. Am. Heart Assoc.* **2018**, *7*, 1. [Crossref]

3. Fernandez, M. L.; Murillo, A. G.; *Nutrients* **2022**, *14*, 2168. [Crossref]

4. Soliman, G. A.; *Nutrients* **2018**, *10*, 780. [Crossref]

5. Dietary Guidelines for Americans Trusted Source, https://health. gov/our-work/nutrition-physical-activity/dietary-guidelines/previous-dietary-guidelines/2015, accessed in March 2023.

6. Kartal, F.; Denizli, A.; *Colloids Surf., B* **2020**, *190*, 110860. [Crossref]

7. Dinh, T. T. N.; Thompson, L. D.; Galyean, M. L.; Brooks, J. C.; Patterson, K. Y.; Boylan, L. M.; *Compr. Rev. Food Sci. Food Saf.* **2011**, *10*, 269. [Crossref]

8. Naviglio, D.; Gallo, M.; le Grottaglie, L.; Scala, C.; Ferrara, L.; Santini, A.; *Food Chem.* **2012**, *132*, 701. [Crossref]

9. Bauer, L. C.; Santana, D. A.; Macedo, M. S.; Torres, A. G.; de Souza, N. E.; Simionato, J. I.; *J. Braz. Chem. Soc.* **2014**, *25*, 161. [Crossref]

10. Al-Hasani, S. M.; Hlavac, J.; Carpenter, M. W.; *J. AOAC Int.* **1993**, *76*, 902. [Crossref]

11. Daneshfar, A.; Khezeli, T.; Lotf, H. J.; *J. Chromatogr. B* **2009**, *877*, 456. [Crossref]

12. Arghavani-Beydokhti, S.; Rajabi, M.; Alireza, A.; *Anal. Bioanal. Chem.* **2017**, *409*, 4395. [Crossref]

13. Nezhadali, A.; Es'haghi, Z.; Khatibi, A. D.; *Food Anal. Methods* **2017**, *10*, 1397. [Crossref]

14. Clausen, D. N.; Visentainer, J. V.; Tarley, C. R. T.; *Analyst* **2014**, *139*, 5021. [Crossref]

15. Puoci, F.; Curcio, M.; Cirillo, G.; Iemma, F.; Spizzirri, U. G.; Picci, N.; *Food Chem.* **2008**, *106*, 836. [Crossref]

16. Turiel, E.; Martín-Esteban, A.; *TrAC, Trends Anal. Chem.* **2019**, *118*, 574. [Crossref]

17. Chen, L.; Wang, X.; Lu, W.; Wu, X.; Li, J.; *Chem. Soc. Rev.* **2016**, *45*, 2137. [Crossref]

18. Malik, M. I.; Shaikh, H.; Mustafa, G.; Bhanger, M. I.; *Sep. Purif. Rev.* **2019**, *48*, 179. [Crossref]

19. Effting, L.; Prete, M. C.; Urbano, A.; Effting, L. M.; González, M. E. C.; Bail, A.; Tarley, C. R. T.; *React. Funct. Polym.* **2022**, *172*, 105178. [Crossref]

20. Ansell, R. J.; Mosbach, K.; *Analyst* **1998**, *123*, 1611. [Crossref]

21. Zhao, W.-R.; Kang, T.-F.; Lu, L.-P.; Cheng, S.-Y.; *RSC Adv.* **2018**, *8*, 13129. [Crossref]

22. Du, L.; Wu, Y.; Zhang, X.; Zhang, F.; Chen, X.; Cheng, Z.; Wu, F.; Tan, K.; *J. Sep. Sci.* **2017**, *40*, 2819. [Crossref]

23. Wang, Y.; Tian, M.; Yu, K.; Li, L.; Zhang, Z.; Li, L.; *New J. Chem.* **2019**, *43*, 3400. [Crossref]

24. He, Y.; Zhao, F.; Zhang, C.; Abd EI-Aty, A. M.; Baranenko, D. A.; Hacimüftüoğlu, A.; She, Y.; *J. Chromatogr. B* **2019**, *1132*, 121811. [Crossref]

25. Tabaraki, R.; Sadeghinejad, N.; *Chem. Pap.* **2020**, *74*, 1937. [Crossref]

26. Liu, Z.; Wang, J.; Wang, Z.; Xu, H.; Di, S.; Zhao, H.; Qi, P.; Wang, X.; *J. Chromatogr. A* **2022**, *1664*, 462789. [Crossref]

27. Kamari, K.; Taheri, A.; *J. Taiwan Inst. Chem. Eng.* **2018**, *86*, 230. [Crossref]

28. Rahmani, M. E.; Ansari, M.; Kazemipour, M.; Nateghi, M.; *J. Sep. Sci.* **2018**, *41*, 958. [Crossref]

29. Mirzapour, F.; Sadeghi, M.; *Iran. Polym. J.* **2022**, *31*, 553. [Crossref]

30. Ansari, S.; *TrAC, Trends Anal. Chem.* **2017**, *90*, 89. [Crossref]

31. Long, G. L.; Winefordner, J. D.; *Anal. Chem.* **1983**, *55*, 712. [Crossref]

32. Nacano, L. R.; Segatelli, M. G.; Tarley, C. R. T.; *J. Braz. Chem. Soc*. **2010**, *21*, 419. [Crossref]

33. Gunnlaugsdottir, H.; Ackaman, R. G.; *J. Sci. Food Agric.* **1992**, *61*, 235. [Crossref]

34. Güney, S.; Güney, O.; *Electroanalysis* **2017**, *29*, 2579. [Crossref]

35. de Mendonça, E. S. D. T.; de Faria, A. C. B.; Dias, S. C. L.; Aragón, F. F. H.; Mantilla, J. C.; Coaquira, J. A. H.; Dias, J. A.; *Surf. Interfaces* **2019**, *14*, 34. [Crossref]

36. Khosroshahi, M. E.; Ghazanfari, L.; *Mater. Sci. Eng.: C* **2012**, *32*, 1043. [Crossref]

37. Wang, X.; Wang, L.; He, X.; Zhang, Y.; Chen, L.; *Talanta* **2009**, *78*, 327. [Crossref]

38. Zhai, C.; Lu, Q.; Chen, X.; Peng, Y.; Chen, L.; Du, S.; *J. Chromatogr. A* **2009**, *1216*, 2254. [Crossref]

39. Polenz, M. F.; Giannina Sante, L. G.; Malschitzky, E.; Bail, A.; *Sustainable Chem. Pharm.* **2022**, *27*, 100678. [Crossref]

40. Li, H.; Li, N.; Jiang, J.; Chen, D.; Xu, Q.; Li, H.; He, J.; Lu, J.; *Sens. Actuators, B* **2017**, *246*, 286. [Crossref]

41. Kumar, B.; Yadav, G. S.; Kumar, N.; Kumar, A.; Raghu, H. V.; *Food Anal. Methods* **2022**, *15*, 1269. [Crossref]

42. Ma, J.; Wu, G.; Li, S.; Tan, W.; Wang, X.; Li, J.; Chen, L.; *J. Chromatogr. A* **2018**, *1553*, 57. [Crossref]

43. Shazly, A. B.; Hassan, L. K.; Kholif, A. E. M.; Sayed, A. F.; El-aziz, M. A.; *Acta Sci.* **2022**, *45*, e58482. [Crossref]

44. Gorban, A. M. S.; Izzeldin, O. M.; *Int. J. Food Sci. Technol.* **1999**, *34*, 229. [Crossref]

45. Pietrzak-Fiecko, R.; Kamelska-Sadowska, A. M.; *Nutrients* **2020**, *12*, 18. [Crossref]

46. Çaktü, K.; Baydemir, G.; Ergün, B.; Yavuz, H.; *Artif. Cells, Nanomed., Biotechnol.* **2014**, *42*, 365. [Crossref]

47. Shi, Y.; Zhang, J.-H.; Jiang, M.; Zhu, Y.-X.; Mei, S.-R.; Zhou, Y.-K.; Dai, K.; Lu, B.; *J. Pharm. Biomed. Anal.* **2006**, *42*, 549. [Crossref]